



OPEN Neural network-based automated proptosis measurement using computed tomography images for patients with thyroid-associated orbitopathy

Sujeong Han¹, Jaesung Lee¹✉ & Jeong Kyu Lee²✉

The purpose of this study was to evaluate the clinical feasibility and reliability of a neural network (NN)-based automated proptosis measurement system using computed tomography (CT) images. An automated proptosis measurement system was developed using the CT images of 200 eyes from 100 patients diagnosed with thyroid-associated orbitopathy. We compared the proptosis value obtained from the proposed automated system with the values obtained from the Hertel exophthalmometer and manual measurements of CT slices. The average measurement values were 17.77 ± 2.47 mm with the Hertel exophthalmometer, 18.87 ± 2.68 mm with the manual measurement of CT slices, and 19.30 ± 2.76 mm with the proposed automated system. There was no significant difference in the proptosis values measured using the manual and automated NN-based methods ($p = 0.241$). The values obtained from manual measurement and automated measurement using CT images showed excellent agreement with an intraclass correlation coefficient of 0.95. Based on the Bland-Altman plots, the 95% limits of agreement between manual CT and NN-based measurements were much smaller than those between Hertel exophthalmometer measurement and manual and NN-based measurements. In conclusion, automated NN-based measurements could provide a straightforward and efficient method for measuring proptosis using CT images.

Keywords Computed tomography, Thyroid-associated orbitopathy, Proptosis, Neural network, Hertel exophthalmometer

Accurate measurement of proptosis is essential for diagnosing orbital diseases such as thyroid-associated orbitopathy¹, orbital fractures, and orbital tumors. There are several methods of measuring proptosis. Among these methods, the Hertel exophthalmometer is the most commonly used tool for measuring proptosis². It measures the vertical distance from the lines connecting both lateral orbital rims to the corneal vertex. However, the Hertel exophthalmometer has limitations in terms of accuracy and reliability due to observer variability^{3,4}. Improperly positioned footplates, inconsistent measurement techniques, and parallax errors can lead to measurement discrepancies^{5,6}. Variability in subjects' characteristics, such as strabismus, asymmetry of the lateral canthi, and soft tissue swelling, may also contribute to the measurement error.

To address existing limitations, computed tomography (CT) images have been utilized to measure the degree of proptosis^{7–10}. However, there are several drawbacks to measuring proptosis using CT images. As the highest point of the cornea and the line connecting the lateral orbital rims cannot always be captured in the same plane on a two-dimensional CT scan, the level of the measured CT slice may not correspond to the area of maximum proptosis. In patients with strabismus, the eyeball may be misaligned either horizontally or vertically, resulting in inaccurate measurements. Manual segmentation of regions of interest, such as the lateral orbital rim and cornea, along with the process of drawing lines between targeted areas, is time-consuming. To address this limitation, several software programs have been developed to semi-automatically measure proptosis in CT images¹¹. However, semi-automated measurements still require manual input, which can prolong the analysis process. Fully automated measurements using automated segmentation algorithms aim to reduce the analysis

¹Department of Artificial Intelligence, Chung-Ang University, Seoul 06974, South Korea. ²Department of Ophthalmology, Chung-Ang University College of Medicine, Chung-Ang University Hospital, 102 Heukseok-ro, Dongjak-gu, Seoul 06973, South Korea. ✉email: curseor@cau.ac.kr; lk1246@gmail.com

time while maintaining consistency. These automated methods are designed to achieve results equivalent to those of manual CT measurements, with improved efficiency.

Recently, neural networks (NNs) have been utilized for image analysis in eyelid and orbital diseases. NNs allow the development of an automated and efficient computer-aided diagnosis system. If appropriate NN techniques can be applied to measuring proptosis using CT images, they could provide more consistent and accurate measurements and significantly reduce the time needed for analysis. A previous study has reported the use of a NN technique in proptosis measurement with CT images¹².

In this study, we proposed a NN-based automated method for measuring proptosis using axial CT images. Our method enhances a previously reported NN model by incorporating a rotation step that aligns the positions of both bones in parallel. This step is crucial as it allows for easier and more accurate calculations by comparing pixel positions and ensuring the proper alignment of the bone ends. In addition, we attempted to assess the performance of the proposed method by comparing it with a manual measurement method using CT images.

Results

A total of 200 eyes from 100 subjects were included in this study. The average age was 35.9 ± 143.2 years. There were 12 male patients and 88 female patients.

To accurately assess the degree of proptosis, it is crucial to choose the most suitable CT slice for measurement. A comparison between the manually selected CT slice for measurement and the CT slice automatically chosen by a NN revealed that the same CT slice was selected for all 100 subjects, indicating 100% agreement.

We compared the proptosis values obtained with the Hertel exophthalmometer, manual measurement of CT axial slices, and proposed automated measurement system using a NN. The average measurement values were 17.77 ± 2.47 mm with the Hertel exophthalmometer, 18.87 ± 2.68 mm with the manual measurement of CT slices, and 19.30 ± 2.76 mm with the proposed automated system. The proptosis value obtained using the Hertel exophthalmometer was 1.0 mm and 1.5 mm lower compared with the values obtained using the manual and NN method, respectively, which was statistically significant ($p < 0.001$, $p < 0.001$). On the contrary, there was no statistically significant difference in the proptosis values measured using the manual and proposed NN method ($p = 0.241$) (Fig. 1).

The values obtained from manual measurement and automated measurement of the degree of proptosis using CT images showed excellent agreement for all subjects. The intraclass correlation coefficient (ICC) was 0.95. On the other hand, the value measured with the Hertel exophthalmometer showed moderate agreement with ICCs of 0.75 and 0.71 compared with the manual CT measurement and NN-assisted measurement values, respectively (Fig. 2).

Based on Bland-Altman plots, the average difference with 95% limits of agreement for the proptosis degree between manual CT measurement and NN-based measurement was 0.42 mm with a range of -1.02 to 1.88 mm.

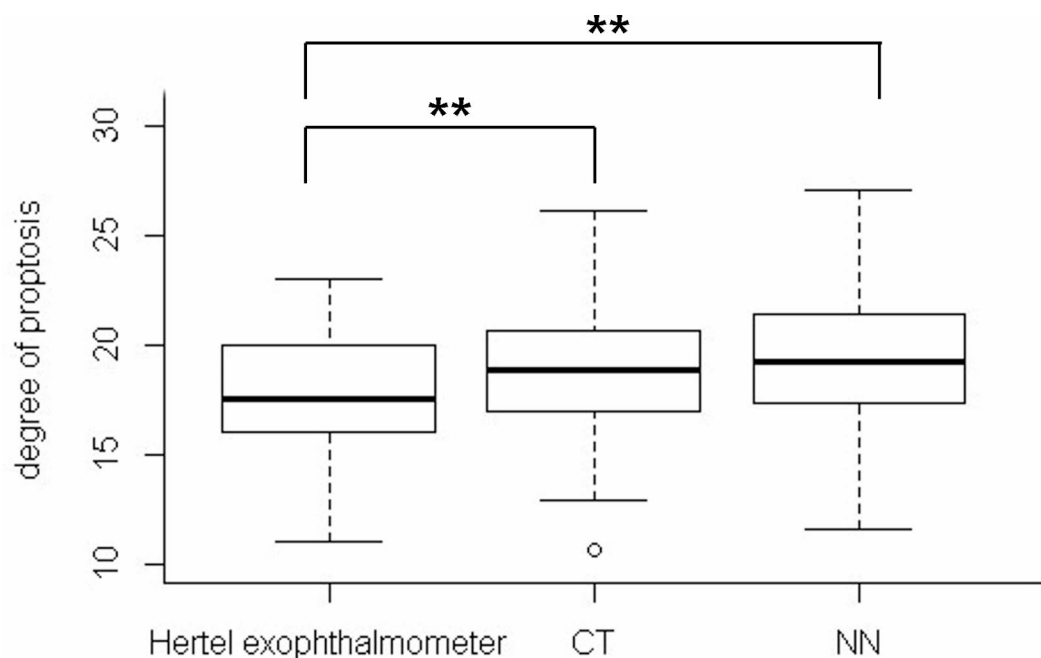


Fig. 1. Comparison of the Hertel exophthalmometer, computed tomography (CT), and neural network (NN)-based method. The proptosis value measured using the Hertel exophthalmometer was 1.0 mm and 1.5 mm lower compared with eh values obtained using the manual and NN methods, respectively, which was statistically significant. However, there was no statistically significant difference in the proptosis values measured using the manual and proposed NN methods. ** < 0.001. Bonferroni correction after repeated measure one-way analysis of variance.

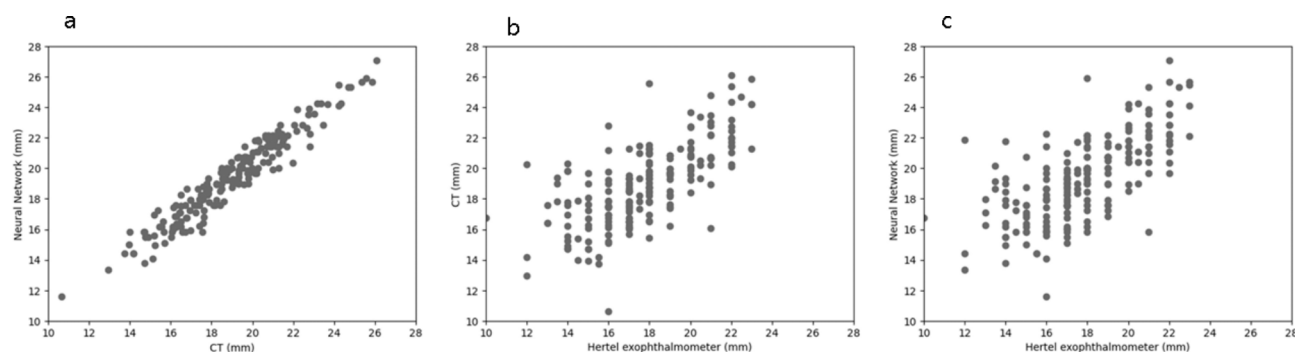


Fig. 2. Correlation between manual computed tomography (CT), neural network (NN)-based, and Hertel exophthalmometer measurements. **(a)** Manual CT measurements and NN-based measurements (intraclass correlation coefficient (ICC)=0.95), **(b)** Hertel exophthalmometer and manual CT measurements (ICC=0.76), and **(c)** Hertel exophthalmometer and NN-based measurements (ICC=0.71).

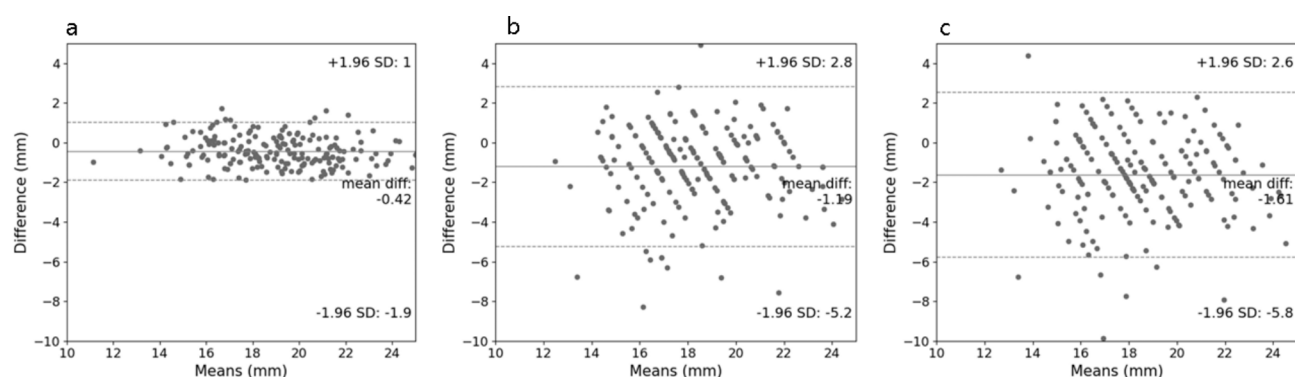


Fig. 3. Bland-Altman plots comparing manual computed tomography (CT), neural network (NN)-based, and Hertel exophthalmometer measurements. **(a)** Manual CT measurements and NN-assisted measurements, **(b)** Hertel exophthalmometer and manual CT measurements, and **(c)** Hertel exophthalmometer and NN-based measurements.

The average differences with 95% limits of agreement for the values between Hertel exophthalmometer measurement and manual CT and NN-based measurements were 1.19 mm with a range of -2.85 to 5.22 mm and 1.61 mm with a range of -2.56 to 5.79 mm, respectively (Fig. 3). To assess the statistical significance of these differences, we conducted the F-test to compare the variances among the measurement methods. A comparison of the variance between manual CT and NN-based measurements with that between manual CT and Hertel exophthalmometer measurements yielded an F-statistic of 54.6085 ($p < 0.001$). Similarly, a comparison of the variance between manual CT and NN-based measurements with that between Hertel exophthalmometry and NN-based measurements resulted in an F-statistic of 23.9609 ($p < 0.001$). These results indicated that the 95% limits of agreement between manual CT and NN-based measurements were significantly smaller than those between Hertel exophthalmometer measurements and both manual CT and NN-based measurements.

Discussion

In this study, we aimed to automatically estimate the degree of proptosis based on the axial view of CT images. Proptosis is a crucial indicator for evaluating the progression and severity of TAO, and it also aids in the diagnosis of orbital diseases^{13,14}. Therefore, the precise clinical assessment of proptosis is essential for diagnosing TAO. However, current methods are constrained by the variability of results related to the clinician^{15,16}. In this study, we proposed an automated method for measuring the degree of proptosis in patients with TAO using NN and image processing techniques, resulting in improved efficiency.

Both our study and previous research, such as that by Zhang et al.¹², employ segmentation NNs to automate the measurement of exophthalmos, highlighting the potential of artificial intelligence in medical imaging. These approaches aim to reduce the subjectivity and variability inherent in traditional manual methods. However, our study includes a novel rotation step to align the positions of both bones in parallel, which simplifies and automates the measurement of proptosis. This additional step distinguishes our method from previous studies. Furthermore, our study provides comprehensive validation by comparing automated measurements not only with manual CT measurements but also with Hertel exophthalmometry, offering a more robust assessment of the system's accuracy.

Our study demonstrated the excellent correlation between manual and NN-based automated measurements of proptosis using CT axial slices. The difference between the two measurements was only 0.43 mm, and the ICC was 0.95. Considering that the NN-based automated method can be much more time-efficient and consistent than the manual method, NN-based measurement could serve as a substitute for manual measurement. In most previous studies that measured proptosis semi-automatically or automatically, the CT axial slice was determined manually. In this study, the slice selection framework was programmed to automatically choose the slice with the largest eyeball. The automatically selected slices were consistent with the manually selected slices. Therefore, in this study, the entire measurement process could be automated with the help of a NN, which is advantageous.

The results showed significant differences between proptosis measurements using the Hertel exophthalmometer and CT methods. The mean values measured manually using CT images and automatically using a NN were 1.0 mm and 1.50 mm longer, respectively, than the value measured using the Hertel exophthalmometer. The proptosis value obtained from CT scans appeared to be higher than that obtained from Hertel exophthalmometry. Previous studies have also reported that proptosis values obtained with CT were 0.30–1.43 mm greater than those obtained with the Hertel exophthalmometer^{11,17}. This difference may be attributed to variations between Hertel exophthalmometry, which is conducted in a sitting position, and CT, which is conducted in a supine position. Furthermore, when using the Hertel exophthalmometer, reference points are located at the back rather than at the footrest due to the presence of skin and soft tissue. The value measured using the Hertel exophthalmometer showed relatively lower correlations with the values measured using the manual and NN-based method, with ICCs of 0.71 and 0.75, respectively. The Hertel exophthalmometer and CT-based methods both measure the distance from both orbital rims to the corneal apex in a similar manner. However, discrepancies in measurement values may arise from variations in the equipment. Therefore, the values measured with the Hertel exophthalmometer and the values measured with CT should not be interchanged.

Our proposed method differs from other existing methods in its approach to data processing and the measurement of the proptosis degree^{18,19}. First, our approach enhanced the efficiency of measuring proptosis by utilizing various image processing techniques. By distinguishing between the colors of the eyeball and the bone, we accurately identified the positions of the ends of the eyeball and the bone based solely on the color information. Additionally, we simplified the process of measuring the degree of proptosis by aligning the ends of the bones to be parallel. This adjustment allows the estimation to rely solely on the positional data of the pixels. Second, with our approach, proptosis degree measurement was possible based on only the difference in the y-coordinates between the end of the bone and the end of the eyeball. Therefore, the degree of proptosis can be measured with less computational effort and time. Third, our method could overcome the limitations of the conventional measurement method for proptosis degree used by clinicians. The traditional approach relies on subjective assessments by clinicians, leading to inconsistency, limited reproducibility, and low accuracy. The proposed method can automatically measure the degree of proptosis using CT images and mask images as input, ensuring consistent and objective results. By applying the eyeball segmentation model utilized in previous image segmentation studies, it is possible to measure the degree of proptosis by inputting CT images, leading to a more automated approach for measuring ocular proptosis.

Our study has several limitations. Similar to most artificial intelligence research, this study is limited by the small number of subjects. Also, the gender distribution in the study was skewed towards more women than men, reflecting the higher prevalence of TAO in women than in men. However, since the study primarily focused on developing techniques for quantifying image values, efforts to balance the gender distribution were not made under the assumption that gender would not significantly impact the study outcomes. The study's exclusive focus on patients with TAO may limit its generalizability and applicability to a broader population. Nevertheless, the fundamental principle of measuring exophthalmos remains consistent across different conditions. It involves the horizontal line connecting both orbital lateral rims to the vertex of each eye. Hence, the NN-based approach proposed for exophthalmos measurement is believed to have broad applicability, encompassing normal individuals, except those with lateral orbital wall fractures or deformities. Additionally, since the measurements were taken by selecting a specific slice from CT images, there is a possibility of inaccuracy in the measurements if the eyes are not properly aligned, especially in case of vertical deviation or when the subject's gaze is not directed straight ahead. Our study could not resolve this existing problem. Therefore, a method of measuring the entire orbit, including the eye, by reconstructing it in three dimensions, can be considered as an alternative. Although this study had inherent limitations in using two-dimensional CT images, a more comprehensive analysis would be possible if three-dimensional images could be used to evaluate exophthalmos. Further research on this topic should be conducted in the near future.

In conclusion, we proposed a NN-based measurement system that could automatically measure the degree of proptosis using CT images. The value obtained with our proposed method demonstrated a strong correlation with the proptosis value manually measured using CT images. With this automated proptosis measurement system, it is possible to consistently and efficiently measure the degree of proptosis in a timely manner. However, there was a significant difference with the value measured with the Hertel exophthalmometer, making comparison difficult. The system we developed could be implemented in a portable device or integrated into existing medical devices for potential clinical use. Nevertheless, additional research would be needed for future clinical applications.

Methods

The Institutional Review Board (IRB) of Chung-Ang University Hospital approved this retrospective study (IRB No. 2402-105-19510). The requirement for informed consent was waived by the IRB of Chung-Ang University Hospital due to the retrospective nature of this study. Image acquisition, processing, and analysis were performed in accordance with the tenets of the Declaration of Helsinki.

Study subjects

A total of 100 patients diagnosed with TAO were recruited. Patients with a history of facial trauma, orbital surgeries, or incomplete CT image sets were excluded. All patients underwent comprehensive ophthalmologic and CT examinations. Clinical records, including age, gender, previous medical history, and degree of proptosis, were collected for review. The degree of proptosis was independently measured by an experienced clinical observer using the Hertel exophthalmometer (Oculus Inc., Wetzlar, Germany) on the day of the CT examination. The reading was taken as the distance between the point on the temporal orbital rim, the deepest palpable point of the angle, and the apex of the cornea. Measurements were recorded to the nearest 0.5 mm.

Manual proptosis measurement using CT images

All patients were scanned with a 256-slice MDCT scanner (Brilliance 256; Philips Medical Systems, Shaker Heights, OH, USA), as previously described¹¹. Orbital CT scans were obtained using contiguous axial slices, with the head positioned parallel to the Frankfurt plane. During CT, patients were instructed to focus on a fixed point. The scanning parameters were as follows: 120 kV, 150 mAs, 64×0.625 mm detector configuration, 1 mm slice thickness, and 1 mm slice increment. We selected the slice with the largest eyeball in the axial plane for measuring proptosis. Proptosis measurement was conducted on the CT images by drawing a horizontal line between the lateral orbital rims on an axial plane, followed by drawing a perpendicular line forward to the posterior surface of the cornea (Fig. 4). The posterior surface of the cornea was chosen because it can be challenging to define the anterior surface of the cornea on CT images. The same examiner repeated the measurements three times, and the average value was used as the measurement value.

Automated proptosis measurement

To measure the proptosis degree using CT images, it is essential to select the slice showing the largest eyeball in the axial view. We selected the largest eyeball slice based on the eyeball segmentation NN from a previous study²⁰. This model was trained to specifically segment the eyeball, excluding surrounding tissues such as retrobulbar fat. First, all slices in the axial view for each patient were resized to 512×512 pixels. Second, all slices were input into the NN to obtain an eyeball mask. Next, the percentage of the eyeball in the entire image was calculated using the eyeball mask obtained through the NN. By applying binarization to the mask and subsequently calculating the ratio of positive pixels to the total number of pixels, the proportion of the eyeball can be quantified efficiently. This ratio was determined by counting the number of pixels that represent the eyeball (value 1) and dividing that by the total number of pixels in the image. Finally, the slice with the largest eyeball proportion was selected for all patients. With an automated eyeball slice selection framework, we can efficiently select the appropriate eyeball slices for proptosis measurement.

We used the same method employed by clinicians to measure the degree of proptosis, with the Hertel exophthalmometer. First, we extracted the bony part of the orbit by adjusting the Hounsfield Unit (HU) value in the original CT image. The bone was extracted based on the 600–3000 HU range. Second, we created a dataset to quantify the degree of proptosis by merging the eyeball mask image with the extracted bone image. In this process, the eyeball and bone were clearly distinguished using different colors. Third, for a more precise measurement of the degree of proptosis, we aligned the ends of the bone in the composite image of the eyeball and bone. To align the ends of both bones, the Y-axis points of both bones were found based on the pixel values. The angle between the straight line and the x-axis was determined by connecting each coordinate. And then,

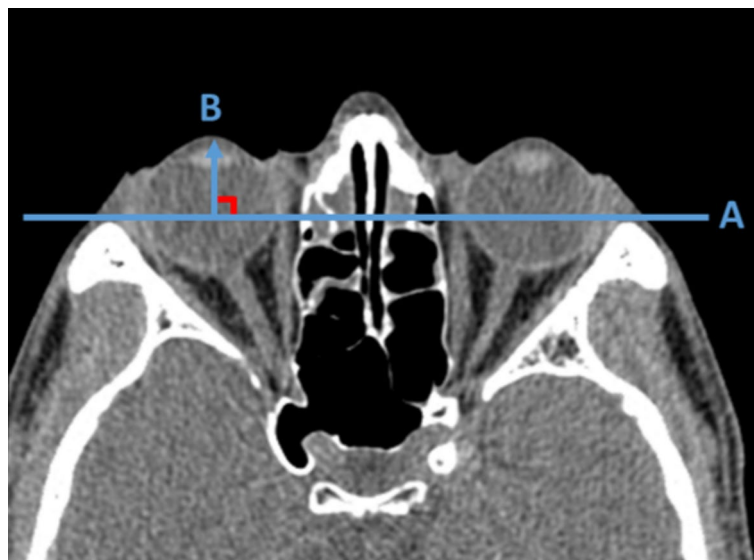


Fig. 4. Manual measurements of proptosis degree using computed tomography (CT) images. A line is drawn between the lateral orbital rims on the axial plane that bisects the lens. Then, Line B is drawn perpendicular to Line A, extending towards the posterior surface of the cornea to measure proptosis.

the coordinates of both ends of the bone were used to extract the radian values by applying the arctan function. Subsequently, the image was rotated by a specific angle so that both ends of the bone were parallel. To assess the degree of proptosis in both eyes, we calculated the absolute difference between the y-coordinates of the endpoints of the bone and the eyeball, which refers to the degree of proptosis in terms of the number of pixels in the CT image. Finally, by multiplying the number of pixels obtained earlier by the pixel unit length, we obtained the estimated value of the proptosis length (Fig. 5). In this process, we utilized the pixel length, which is a piece of metadata extracted from the CT image.

Statistical analysis

Data are expressed as the mean \pm standard deviation. Repeated measures one-way analysis of variance (RM-ANOVA) with Bonferroni correction was used to compare proptosis measurements obtained by different modalities. The ICC was calculated to evaluate the agreement between manual and automated measurements. Bland-Altman plots were used to visualize the discrepancies between manual and automated measurements. As the 95% limits of the Bland-Altman plots are determined by the variance, we conducted the F-test to compare the differences in the 95% limits of the Bland-Altman plots. The 95% confidence intervals for the mean difference and limits of agreement are shown on the plots. All statistical analyses were performed using R software (version 4.2.2). A *p* value less than 0.05 was considered statistically significant.

Data availability

Datasets used and analyzed during the current study are available from the corresponding author upon reasonable request.

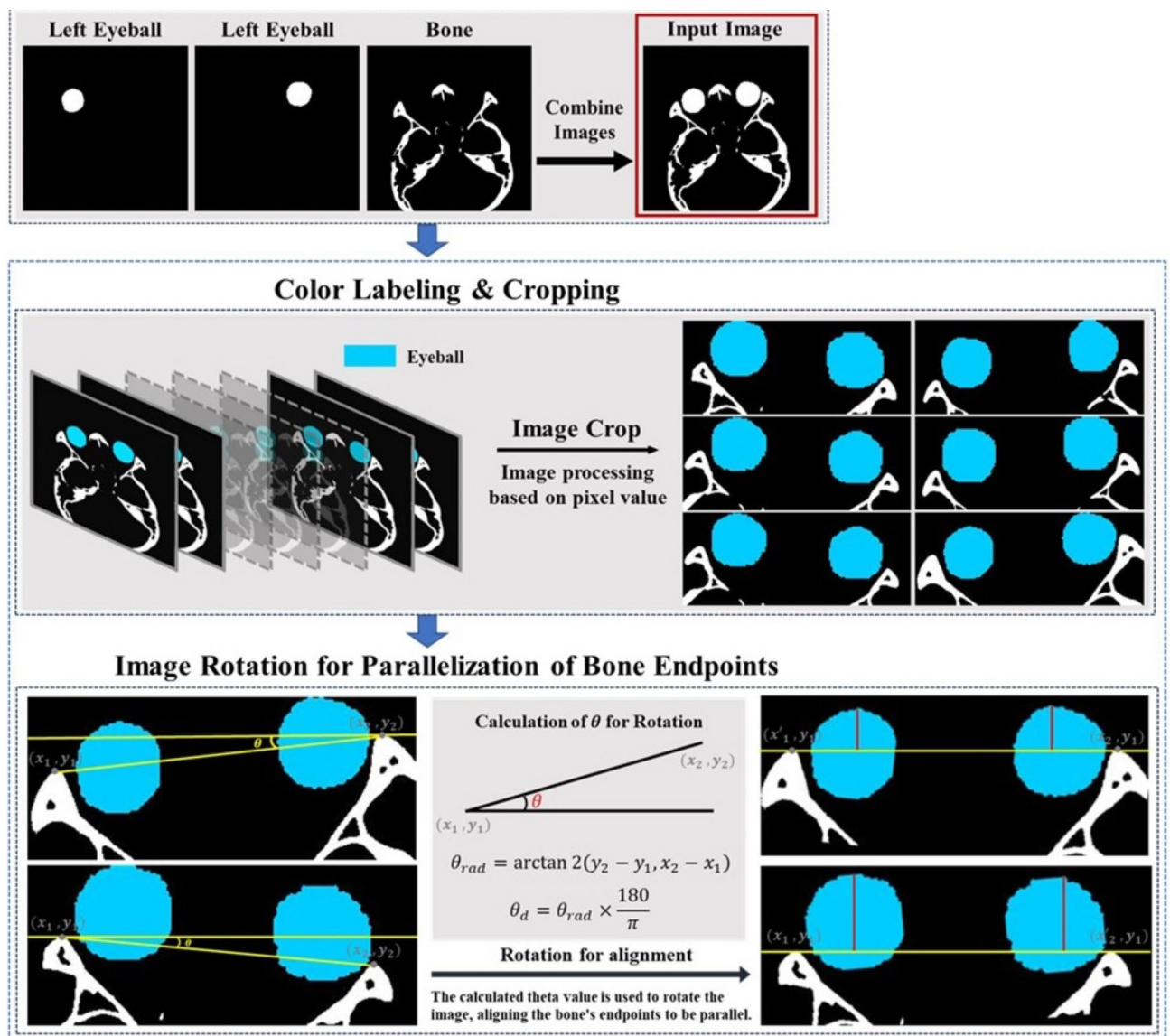


Fig. 5. Overview of neural network-assisted estimation of the proptosis degree.

Received: 15 April 2024; Accepted: 31 October 2024

Published online: 08 November 2024

References

1. Zhu, X. et al. Calculation of ophthalmic diagnostic parameters on a single eye image based on deep neural network. *Multimed. Tools Appl.* **81**, 2311–2331. <https://doi.org/10.1007/s11042-021-11047-z> (2022).
2. Migliori, M. E. & Gladstone, G. J. Determination of the normal range of exophthalmometric values for black and white adults. *Am. J. Ophthalmol.* **98**, 438–442. [https://doi.org/10.1016/0002-9394\(84\)90127-2](https://doi.org/10.1016/0002-9394(84)90127-2) (1984).
3. O'Donnell, N. P., Virdi, M. & Kemp, E. G. Hertel exophthalmometry: the most appropriate measuring technique. *Br. J. Ophthalmol.* **83**, 1096b. <https://doi.org/10.1136/bjo.83.9.1096b> (1999).
4. Kashkoui, M. B., Beigi, B., Noorani, M. M. & Nojoomi, M. Hertel exophthalmometry: reliability and interobserver variation. *Orbit* **22**, 239–245. <https://doi.org/10.1076/orbi.22.4.239.17245> (2003).
5. Frueh, B. R., Garber, F., Grill, R. & Musch, D. C. Positional effects on exophthalmometer readings in Graves' eye disease. *Arch. Ophthalmol.* **103**, 1355–1356. <https://doi.org/10.1001/archophth.1985.01050090107043> (1985).
6. Ameri, H. & Fenton, S. Comparison of unilateral and simultaneous bilateral measurement of the globe position, using the Hertel exophthalmometer. *Ophthalmic Plast. Reconstr. Surg.* **20**, 448–451. <https://doi.org/10.1097/01.iop.0000143712.42344.8c> (2004).
7. Hallin, E. S. & Feldon, S. E. Graves' ophthalmopathy: II. Correlation of clinical signs with measures derived from computed tomography. *Br. J. Ophthalmol.* **72**, 678–682. <https://doi.org/10.1136/bjo.72.9.678> (1988).
8. Segni, M., Bartley, G. B., Garrity, J. A., Bergstralh, E. J. & Gorman, C. A. Comparability of proptosis measurements by different techniques. *Am. J. Ophthalmol.* **133**, 813–818. [https://doi.org/10.1016/s0002-9394\(02\)01429-0](https://doi.org/10.1016/s0002-9394(02)01429-0) (2002).
9. Nkenke, E. et al. Hertel exophthalmometry versus computed tomography and optical 3D imaging for the determination of the globe position in zygomatic fractures. *Int. J. Oral Maxillofac. Surg.* **33**, 125–133. <https://doi.org/10.1054/ijom.2002.0481> (2004).
10. Park, N. R., Moon, J. H. & Lee, J. K. Hertel exophthalmometer versus computed tomography scan in proptosis estimation in thyroid-associated orbitopathy. *Clin. Ophthalmol.* **13**, 1461–1467. <https://doi.org/10.2147/ophth.S216838> (2019).
11. Huh, J., Park, S. J. & Lee, J. K. Measurement of proptosis using computed tomography based three-dimensional reconstruction software in patients with Graves' orbitopathy. *Sci. Rep.* **10**, 14554. <https://doi.org/10.1038/s41598-020-71098-4> (2020).
12. Zhang, Y. et al. Automatic measurement of exophthalmos based orbital CT images using deep learning. *Front. Cell. Dev. Biol.* **11**, 1135959. <https://doi.org/10.3389/fcell.2023.1135959> (2023).
13. Sawicka-Gutaj, N. et al. Eye symptoms in patients with benign thyroid diseases. *Sci. Rep.* **11**, 18706. <https://doi.org/10.1038/s41598-021-98232-0> (2021).
14. Bartalena, L., Pinchera, A. & Marcocci, C. Management of Graves' ophthalmopathy: reality and perspectives. *Endocr. Rev.* **21**, 168–199. <https://doi.org/10.1210/edrv.21.2.0393> (2000).
15. Sleep, T. J. & Manners, R. M. Interinstrument variability in Hertel-type exophthalmometers. *Ophthalmic Plast. Reconstr. Surg.* **18**, 254–257. <https://doi.org/10.1097/00002341-200207000-00004> (2002).
16. Chang, A. A., Bank, A., Francis, I. C. & Kappagoda, M. B. Clinical exophthalmometry: a comparative study of the Luedde and Hertel exophthalmometers. *Aust. N. Z. J. Ophthalmol.* **23**, 315–318. <https://doi.org/10.1111/j.1442-9071.1995.tb00182.x> (1995).
17. Kim, I. T. & Choi, J. B. Normal range of exophthalmos values on orbit computerized tomography in Koreans. *Ophthalmologica* **215**, 156–162. <https://doi.org/10.1159/000050850> (2001).
18. Campi, I. et al. A quantitative method for assessing the degree of axial proptosis in relation to orbital tissue involvement in Graves' orbitopathy. *Ophthalmology* **120**, 1092–1098. <https://doi.org/10.1016/j.ophtha.2012.10.041> (2013).
19. Mourits, M. P., Lombardo, S. H., van der Sluijs, F. A. & Fenton, S. Reliability of exophthalmos measurement and the exophthalmometry value distribution in a healthy Dutch population and in Graves' patients. An exploratory study. *Orbit* **23**, 161–168. <https://doi.org/10.1080/01676830490504089> (2004).
20. Lee, S. H., Lee, S., Lee, J., Lee, J. K. & Moon, N. J. Effective encoder-decoder neural network for segmentation of orbital tissue in computed tomography images of Graves' orbitopathy patients. *PLoS One* **18**, e0285488. <https://doi.org/10.1371/journal.pone.0285488> (2023).

Acknowledgements

This research was supported by the National Research Foundation of Korea (NRF) grant funded by the Korea government (MSIT) (NRF-2021R1A2C1011351) and Institute of Information & Communications Technology Planning & Evaluation (IITP) grant funded by the Korean government (MSIT) (2021-0-01341, Artificial Intelligence Graduate School Program (Chung-Ang University)). The funding organization had no role in the design or conduct of this research. The authors would like to thank Subin Jang for statistical analysis.

Author contributions

J.K.L. and J.L. devised the project and the main conceptual ideas. S.H. collected and analyzed the data. S.H., J.K.L. and J.L. wrote the manuscript.

Declarations

Competing interests

The authors declare no competing interests.

Additional information

Correspondence and requests for materials should be addressed to J.L. or J.K.L.

Reprints and permissions information is available at www.nature.com/reprints.

Publisher's note Springer Nature remains neutral with regard to jurisdictional claims in published maps and institutional affiliations.

Open Access This article is licensed under a Creative Commons Attribution-NonCommercial-NoDerivatives 4.0 International License, which permits any non-commercial use, sharing, distribution and reproduction in any medium or format, as long as you give appropriate credit to the original author(s) and the source, provide a link to the Creative Commons licence, and indicate if you modified the licensed material. You do not have permission under this licence to share adapted material derived from this article or parts of it. The images or other third party material in this article are included in the article's Creative Commons licence, unless indicated otherwise in a credit line to the material. If material is not included in the article's Creative Commons licence and your intended use is not permitted by statutory regulation or exceeds the permitted use, you will need to obtain permission directly from the copyright holder. To view a copy of this licence, visit <http://creativecommons.org/licenses/by-nc-nd/4.0/>.

© The Author(s) 2024